Ionization thermodynamics of poly(acrylic acid) in ionic liquids

Ryo Kanzaki, Clément Guibert, Jérôme Fresnais, Véronique Peyre

Journal of Molecular Liquids 437 (2025) 128261

Contents lists available at ScienceDirect

Journal of Molecular Liquids

journal homepage: www.elsevier.com/locate/molliq

Ionization thermodynamics of poly(acrylic acid) in ionic liquids

Ryo Kanzaki [a,*], Clément Guibert [b], Jérôme Fresnais [c], Véronique Peyre [c]

[a] Graduate School of Science and Engineering, Kagoshima University, 1-21-35 Korimoto, Kagoshima 890-0065, Japan
[b] Sorbonne Université, CNRS, Laboratoire de Réactivité de Surface, LRS, F-75005 Paris, France
[c] Sorbonne Université, CNRS, Laboratoire Physico-Chimie des Electrolytes et des Nanosystèmes Interfaciaux, PHENIX, F-75005 Paris, France

ARTICLE INFO

Keywords:
Protic ionic liquid
Polyelectrolyte
Heats of ionization
Potentiometry
Calorimetry

ABSTRACT

The pH response of poly(acrylic acid) (pAA) in protic ionic liquids (PILs), ethylammonium nitrate and diethylethanolammonium trifluoromethanesulfonate, was investigated through potentiometric and calorimetric titrations. The ionization equilibrium of pAA in the PILs, as well as in aqueous solution, was described by a unified model that was modified by adding two parameters to the ionization equilibrium of acetic acid. This model was also consistently applicable to the interpretation of the ionization of nanoparticles coated with pAA (CNp), which allowed the quantitative comparison of the ionization behavior among acetic acid monomer, isolated pAA, and pAA on the CNp surface in each solvent. Furthermore, the origin of these differences was separated into enthalpic and entropic contributions, which enabled a more detailed elucidation of the aggregation and dispersion mechanisms of CNps in ionic liquids. As a result, it was found that the CNp dispersion in ionic liquids at a low degree of ionization is promoted by the entropic factor arising from the release of solvent ions, while the difference between the ionic liquids is primarily due to the enthalpic factor related to hydrogen bonding. When the degree of ionization increased, the effect of ionic liquids as electrolytes on polyelectrolytes became apparent, and a marked difference was observed between EAN and PIL18. In contrast, the thermodynamic enthalpies related to ionization exhibited no significant differences among acetic acid monomer, pAA, and CNp surface pAA, indicating that the ionization of carboxy groups is essentially governed by the acid-base properties of the solvents.

1. Introduction

Ionic liquids are liquids composed only of electrolytes. Their desirable physicochemical characteristics make them a potential alternative to molecular solvents. One of the unique features is that ionic liquids are electrolyte solutions that are concentrated to the limit with no solvent species, and from this perspective, ionic liquids can be regarded as solvents with extremely high ionic strength. Since the cohesive energy stems from electrostatic attractive force, ionic liquids are classified into a distinct category differentiated from conventional solvents, including water and organic solvents [1–4]. We are particularly intrigued by ionic liquids as solvents that offer an exceptional chemical reaction field. Within this framework, we have observed some unique behaviors, such as an athermal metal ion-anionic ligand exchange and a concentration-independent ionic activity coefficient [5,6]. Ionic liquids made of onium salts are called protic ionic liquids (PILs). Like amphoteric solvents, such as water, PILs display simultaneously both the H^+ donating and H^+ accepting abilities because of their cations and anions, respectively. This property allows PILs to be acid-base reaction media. The acid-base character and subsequent effective pH of PILs [7–14] are the fundamental properties that control the dissociation or ionization of electrolytes. Some of our experiences of ionization thermodynamics in PILs have shown that the acid-base properties of PILs tend to reflect those of the constituent ions in aqueous solution.

Another interest in ionic liquids is their use as colloid-dispersing media [15–19]. When the colloids are stabilized by electrostatic repulsions, adding salts induces a reduction in colloidal stability. Indeed, the DLVO theory predicts a monotonic decrease in inter-particle repulsion with increasing ionic strength due to electrostatic screening. Considering this, ionic liquids cannot be considered as “good” dispersing media for charged colloids because they are extremely concentrated electrolyte solutions. However, stable dispersions have been obtained in various ionic liquids, implying the presence of an alternative stabilization mechanism different from conventional electrostatic repulsions [20–26]. Using nanoparticles coated with poly(acrylic acid) (pAA), we have so far demonstrated that the colloidal stability can be tuned by pH in protic ionic liquids, with stable dispersions in acidic and basic conditions and flocculation at intermediate pH. It has been suggested that at

* Corresponding author.
E-mail address: kanzaki@sci.kagoshima-u.ac.jp (R. Kanzaki).

https://doi.org/10.1016/j.molliq.2025.128261
Received 2 April 2025; Received in revised form 24 June 2025; Accepted 30 July 2025
Available online 5 August 2025

least two distinct mechanisms work to stabilize nanoparticle dispersions: (i) the formation of solvation layers, possibly through hydrogen bonds between neutralized surface pAA and the solvent ions at low degree of ionization (α) under acidic conditions, and (ii) electrostatic repulsion overcoming the electrostatic shielding by solvent ions at high α under basic conditions. However, the mechanisms underlying the formation of these protective layers, and how the initial charge of the particles and the nature of the surrounding ionic species can influence them, are still under discussion.

One promising approach to elucidate the CNp stabilization mechanism in ionic liquids is to investigate the ionization behavior of pAA, as it significantly influences interparticle interactions. However, it should be noted that the ionization equilibrium of polyelectrolytes becomes significantly more complex in highly concentrated electrolyte in aqueous systems, and even more in ionic liquids. Given that ionic liquids are considered to be an extremely concentrated electrolyte solution, understanding polyelectrolyte behavior is expected to be more challenging. Nevertheless, information on the ionization thermodynamics of pAA in ionic liquids remains scarce, making this topic itself an interesting subject of investigation. In the current study, we focus on the ionization thermodynamics of pAA in ionic liquids and investigate the effect of the ionization thermodynamic properties on colloidal stability.

2. Experimental

Ionic liquids were synthesized by a neutralization method [27,28]. Solutions of nitric acid and ethylamine (both 70 %, Kanto Kagaku, Japan) were mixed with vigorous stirring in an antifreeze fluid bath at less than 0 °C until the solution reached a mildly acidic condition (pH = 5 on universal pH indicating paper). The mixture was dried in vacuo at 60 °C until 100 ppm of water content, determined by Karl-Fischer Coulombic titrator (APB-620, Kyoto Electronics Manufacturing), to obtain ethylammonium nitrate (EAN). A 1:1 solution (by volume) of trifluoromethanesulfonic acid (TfOH; Sigma-Aldrich, 99 %) was added dropwise into a 1:1 solution (by volume) of distilled *N*,*N*-diethylethanolamine (DEEA; Sigma-Aldrich, 99.5 %) in an antifreeze fluid bath at less than 0 °C until the solution reached a mildly acidic condition (pH = 5 on universal pH indicating paper), followed by freeze-drying for a few weeks. The water content of the obtained ionic liquid [$DEEAH^+$] [TfO^-] (*N*,*N*-diethylethanolammonium triflate) was 800 ppm. Hereafter, this PIL is referred to as PIL18, as the same compound was also used in our previous publication in 2018 [28].

Polyacrylic acid sodium salt (2100 g/mol, Sigma-Aldrich) was dried at 120 °C for a few days. Subsequently, the amount of dissociable (ionizable) carboxy groups, defined hereafter as Y, was determined separately through neutralization titration with an HCl solution. Size-sorted maghemite nanoparticles coated with pAA (coated nanoparticles, hereafter referred to as CNps) were prepared as previously published [28]. Briefly, the fraction of the maghemite nanoparticle with an average hydrodynamic radius of 5 nm characterized in water by DLS (Zetasizer Nano ZS, Malvern) was coated with pAA through the precipitation-redispersion technique to obtain CNps with an average hydrodynamic radius of 9 nm. As reported in detail elsewhere, [28] the main features of the CNps used in this study are as follows: the core diameter determined by TEM was 6.9 nm; SAXS analysis yielded a core size of 6.0 nm with an estimated pAA layer thickness of 0.7 nm; and the surface density of ionizable carboxy groups was approximately 20 nm^{-2}. The aqueous dispersion was added into mildly basic ionic liquids, followed by freeze-drying for water removal to introduce CNps into ionic liquids.

Potentiometric titration was performed with an IS-FET pH electrode (0040-10D, HORIBA, Japan) at 25 °C. The output voltage of IS-FET, *E*, obeys the Nernst equation.

$$E = E_0 + 59.16\ \text{mV} \times \log\left(\frac{[H^+]}{\text{mol dm}^{-3}}\right) \quad (1)$$

where E_0 is the formal potential of this electrode, determined separately by neutralization titration in each solvent. $[H^+]$ denotes the molar concentration of H_3O^+ in water, of HNO_3 in EAN, or of TfOH in PIL18, respectively. The fluctuation in the IS-FET output was within 0.1 mV in most of the pH region analyzed, even in the turbid solution (where CNps are aggregating). The degree of ionization, α, of pAA or CNp can be obtained as follows.

$$\alpha = 1 - \frac{C_H - [H^+] + \frac{K_{AP}}{[H^+]}}{C_Y} \quad (2)$$

where C_H and C_Y represent the total molar concentrations of H^+ and Y (the ionizable carboxy group of pAA) in the sample solution, respectively, and K_{AP} denotes the autoprotolysis constant of the solvent. C_H is given by: $C_H = C_{HA} - C_B + \delta_H$, where C_{HA} and C_B are the added concentrations of acids and bases, respectively, and δ_H is the excess concentration of acid present in the synthesized ionic liquids, which was determined separately through neutralization titrations. The K_{AP} values were also determined for each batch of the synthesized ionic liquids, showing slight fluctuation across batches. Typically, 3 cm^3 of a sample solution containing 0.02 mol dm^{-3} of Y, the ionizable carboxy group, was placed in the thermostated glass cell, which was titrated by 0.1 mol dm^{-3} acidic or basic titrant solution added with an autoburette (APB series, Kyoto Electronics Manufacturing, Japan).

Calorimetric titration was performed with an isoperibol-type lab-made titration calorimeter at 25 °C. Details of the equipment have been described elsewhere [28–30]. Typically, 2.5 cm^3 of the sample solution containing 0.02 mol dm^{-3} of Y was placed in the vessel, which was titrated by 0.2 mol dm^{-3} acidic or basic titrant solution added with a syringe pump (Harvard Model-11 plus). The heat capacity of the vessel was determined before and after each titration series by referring to the Joule heat generated by the electric resistance immersed in the test solution.

3. Results and discussion

3.1. Ionization equilibrium

3.1.1. Poly(acrylic acid) in water

Fig. 1(a) shows the degree of ionization of pAA, α, as a function of pH (hereafter, $pH = -\log\frac{[H^+]}{\text{mol dm}^{-3}}$ is used instead of the formal definition, $pH = -\log a_H$) in aqueous solution (0.1 mol dm^{-3} NaCl). Data are shown in filled symbols. Titrations were repeated three times and presented by different symbols, showing excellent reproducibility. The dashed line expresses the ionization profile of acetic acid calculated using the pK_a value in each solvent determined separately. As shown in this Figure, pAA begins to be ionized at a similar pH to that of acetic acid. This implies that, when pAA is not ionized, the acidity of the polymer carboxy group is almost equal to that of acetic acid. With increasing pH, the α value increases, whereas the ionization of pAA is hindered and the increase in α is less steep than that of acetic acid. Some models have been proposed for pAA ionization [31–38]. We adopted a model in which the apparent ionization constant of pAA depends on its degree of ionization as follows. The apparent ionization constant of pAA, $pK_{a,app}$, can be calculated from experimental data ($[H^+]$ and α) in each titration point using the following equation.

$$pK_{a,app} = -\log\left(\frac{[H^+]}{\text{mol dm}^{-3}}\frac{\alpha}{1-\alpha}\right) \quad (3)$$

where $[H^+]$ and α are given according to Eqs. (1) and (2). For acetic acid, this value remains constant and the value is the ionization constant ($pK_{a,AcOH}$) in each solvent. In case of pAA, this value varies depending on α. Thus, we express the difference between $pK_{a,app}$ and $pK_{a,AcOH}$ using two parameters concerning:

(i) β_0: the shift in the acidity of the carboxy group of pAA when pAA

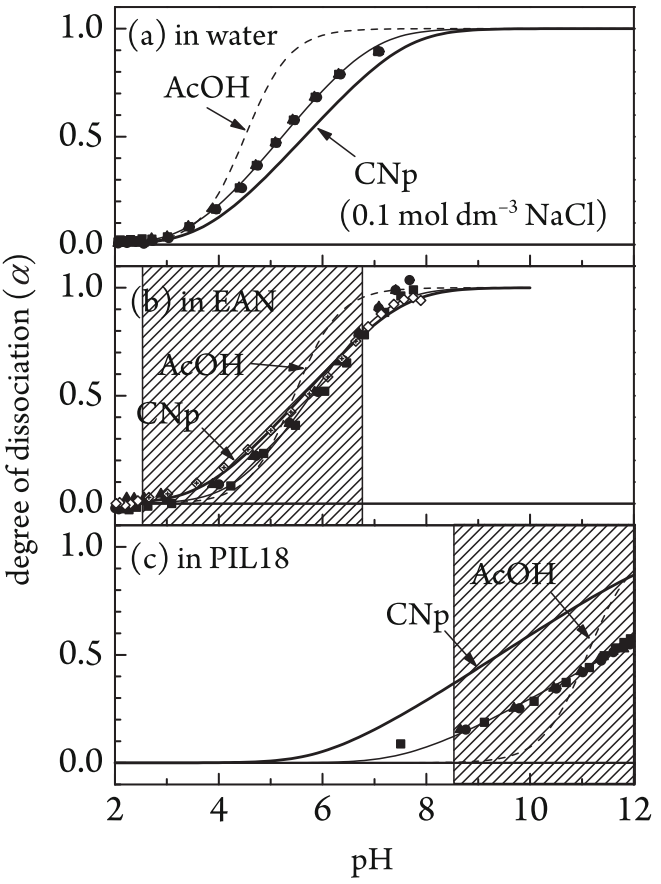

Fig. 1. Potentiometric titration curves of (a) pAA in water (0.1 mol dm^{-3} NaCl), (b) pAA in EAN (filled symbols) and CNp (open symbols), and (c) pAA in PIL18, plotted as the degree of dissociation (α) as a function of pH $\left(=-\log\frac{[H^+]}{\text{mol dm}^{-3}}\right)$. The dotted open symbols in (b) and the shaded pH ranges in (b) and (c) indicate that the CNp solution appears turbid. The solid lines are the theoretical curves calculated using eqs. (3) and (4) with the equilibrium parameters listed in Table 1 (see text); thin lines represent pAA and bold lines represent CNp. The dashed lines show the theoretical ionization curves of acetic acid (AcOH), calculated using the pK_a value in each solvent. Different symbol shapes indicate different repetitions of the titration.

is not ionized (at α = 0) and.

(ii) β_1: the extent of ionization inhibition with increasing α, as follows:

$$pK_{a,app} = pK_{a,AcOH} + \beta_0 + \beta_1\alpha \quad (4)$$

In this model, β_1 is interpreted as reflecting the effect of the electrostatic potential in the vicinity of the pAA chains generated upon ionization, and a parameter with the same physicochemical meaning was introduced in previous studies to describe the polyelectrolyte effect [31–35]. In contrast, β_0 accounts for solvent-specific effects and is introduced in the present work.

The observation shown in Fig. 1(a), namely that the ionization of acetic acid and pAA begins at the same pH (i.e., α starts to increase), suggests a negligible β_0 value and an intrinsically similar acidity of the carboxy group of pAA to that of acetic acid. On the other hand, as α increases with increasing pH, the ionization curve of pAA lies below the theoretical curve of acetic acid. This effect is described as a decrease in the acidity, reflected by an increase in the p$K_{a,app}$ value, where β_1 is the corresponding coefficient (β_1 represents the displacement of p$K_{a,app}$ at α = 1). For monomer monoacids, $\beta_1 = 0$ is expected, meaning that p$K_{a,app}$ remains constant and does not depend on α. These two parameters, β_0 and β_1, are obtained by the least squares fittings. The optimized values in 0.1 mol dm^{-3} NaCl aqueous solutions were $\beta_0 = -0.19$ (separately determined p$K_{a,AcOH} = 4.51$) and $\beta_1 = 1.8$. The theoretical curve using these values is shown as a solid thin line for pAA in Fig. 1(a). Since this line reproduces the experimental points well, Eq. (4) can satisfactorily model the ionization equilibrium of pAA in water.

3.1.2. Poly(acrylic acid) in ionic liquids

Figs. 1(b) and 1(c) show the α vs. pH curves of pAA in EAN and PIL18 ([DEEAH$^+$][TfO$^-$]), respectively, in filled symbols. The dashed line expresses the ionization profile of acetic acid calculated using p$K_{a,AcOH}$ in the respective solvent. In each solvent, the least squares parameter fitting according to Eq. (4) was performed to determine β_0 and β_1 values. The solid thin lines are the theoretical curves using these parameters, reproducing the experimental points well. The parameters determined by least squares fitting in each solvent are summarized in Table 1. Since a consistent model is applicable to pAA regardless of the solvents, the parameters in Eq. (4) allow for a quantitative comparison of interactions between pAA and the solvents. For instance, because of the stronger acidity of the proton carrier in EAN (HNO_3) than that in water (H_3O^+), the ionization of acetic acid occurs at a lower concentration [H^+] (higher pH) in EAN compared to water, resulting in an increase in p$K_{a,AcOH}$ [27]. However, as shown in Fig. 1(b), pAA and acetic acid began to be ionized at almost the same pH. This indicates that the intrinsic acidity of the carboxy group of pAA is similar to that of acetic acid at $\alpha = 0$ when the solvent is EAN. This leads to the relatively small value of β_0 in EAN. In contrast, as shown in Fig. 1(c), the ionization of pAA began at a much lower pH than that of acetic acid in PIL18, unlike in water and EAN. This indicates that the ionization of the carboxy group of pAA is promoted in PIL18 (at $\alpha = 0$) compared to acetic acid. The significantly negative β_0 value reflects this. Thus, β_0 facilitates the evaluation of the ionization equilibrium of pAA, regardless of the acid-base properties of the solvent side.

With increasing pH, the degree of ionization (α) rises, while the ionization is hindered compared to acetic acid, as also observed in water. The extent of this hindrance depends on the solvent, which is quantified by the parameter β_1. The β_1 value is slightly smaller in EAN than in water. This trend is consistent with the previously reported electrolyte effect on pAA in electrolyte solutions [32]. Nevertheless, in both water and EAN, this effect is so minor that α can approach nearly 1, as shown in Figs. 1(a) and 1(b). In contrast, as shown in Fig. 1(c), the ionization of pAA is strongly hindered, resulting in the α value remaining at about 0.5. This is reflected in the remarkably large β_1 value (5.7) compared to that in water and EAN.

3.1.3. Poly(acrylic acid)-coated nanoparticles

We have previously demonstrated that the ionization equilibrium of CNp (pAA on the CNp surface) can also be described by Eq. (4) in water [29]. In Fig. 1(a), the theoretical thick line for CNp using the previously reported parameters ($\beta_0 = 0.05$, $\beta_1 = 2.2$; these values are listed in Table 1) is shown. Since Eq. (4) works for CNp, a similar mechanism, even though the geometry differs, is implied to describe the vicinity of the pAA chains at the surface of the CNp. As shown in Fig. 1(a), both CNp and pAA begin to be ionized at a similar pH at which the ionization of acetic acid begins, indicating the acidity of carboxy groups of pAA and

Table 1
Parameters for ionization equilibria (4) of pAA and CNp in water (0.1 mol dm^{-1} NaCl), EAN and PIL18.

	AcOH	pAA			CNp		
	pK_a	β_1	β_0	pK_{AP}	β_1	β_0	pK_{AP}
water	4.51	1.8	−0.19	14	2.2	0.05	14
EAN	5.45[a]	1.3	−0.31	10.22	2.1	−0.89	9.86
PIL18	11.1[b]	5.7	−2.4	14.3	4.8[b] 7.5[c]	−4.1[b]	14.9[b]

a) Ref. 27, b) Ref. 29, c) Ref. 28

the CNp surface pAA is similar to that of acetic acid at low α and low pH. In fact, a small value of β_0 is obtained for CNp. On the other hand, the hindrance of the α value of CNp at high pH is similar but a little more significant than that of pAA, leading to slightly larger β_1 value for CNp than that for pAA. While minor differences in β are observed, the ionization behavior of pAA on the CNp surface pAA is essentially similar to that of isolated pAA freely dispersed in water.

In contrast, CNp exhibits a different behavior in EAN. The potentiometric titration curve of CNp is shown by open symbols in Fig. 1(b). The dotted open symbols indicate that the sample was turbid, indicating flocculation. Even in the flocculation region, rapid pH response was observed. It was difficult to detect by eyes the switching of flocculation and redispersion at low pH, possibly relating to the shallow slope of the α vs. pH curve. Nevertheless, the solution was transparent dark brown at low enough pH, indicating that CNps were well dispersed. The pH at which CNp began to ionize was shifted to a lower (more acidic) region compared to acetic acid and pAA. For instance, a non-negligible quantity of CNps is ionized ($\alpha > 0.1$) at pH = 4, where the ionization of acetic acid (dashed line) is almost suppressed. Reflecting this, a clearly smaller β_0 value ($\beta_0 = -0.89$) than that in aqueous solution was obtained. In contrast, the β_1 value ($\beta_1 = 2.1$) was similar to that in water.

A similar but more significant behavior of CNp has previously been reported in PIL18 [29]. The calculation curve of CNp ionization ($\beta_0 = -4.1$ and $\beta_1 = 4.8$, Table 1) is shown by a thick line in Fig. 1(c). CNp ionization begins at a much lower pH than that of acetic acid, which is reflected in the large and negative β_0 value of CNp in PIL18. On the other hand, the α vs. pH curve exhibits a gradual slope, suggesting that the ionization of CNp is hindered as α increases, similar to that of pAA. These β values thus enable a quantitative comparison of the behavior of pAA and CNp in the respective solvents.

3.2. Heats of ionization

3.2.1. In water

Fig. 2 shows the results of calorimetric titration of pAA in 0.1 mol dm^{-1} NaCl aqueous solutions. The filled symbols represent the titration profile for the protonation process of sodium salt of pAA titrated with HCl solution. The y-axis is the apparent molar heat of reaction, $Q_{m,app}$, in kJ/mol,

$$Q_{m,app} = \frac{q_{r,i}}{C_T(v_i - v_{i-1})} \tag{5}$$

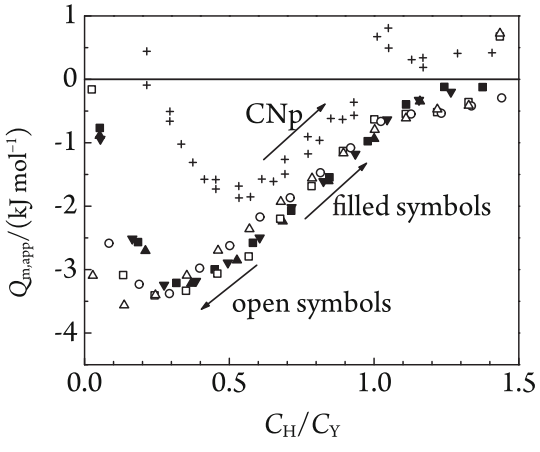

Fig. 2. Calorimetric titration curves of pAA in water (0.1 mol dm^{-3} NaCl), represented in apparent molar heat of reaction, $Q_{m,app}$. Filled symbols indicate the titration of pAA sodium salt with HCl; open symbols indicate the titration of acidified pAA solution with NaOH. The arrows indicate the direction of the titration. The titration points for CNp, shown as cross marks, are included as a reference [29]. Different symbol shapes indicate different repetitions of the titration.

where $q_{r,i}$ is the total heat generated during each injection of the titrant, C_T is the molar concentration of the titrant (HCl), and v_i is the volume of the sample solution at the i-th titration point. The x-axis is the titration ratio C_H/C_Y *after* each injection, where C_H and C_Y are the formal concentrations of HCl and Y (the ionizable carboxy group of pAA in the solution), respectively, and C_H/C_Y increases with the progress of the titration. The negative value of $q_{r,i}$, as shown in Fig. 2 (i.e., $Q_{m,app} < 0$), indicates that the *protonation* of Y^- (reaction 6) of pAA is endothermic.

$$Y^- + H^+ \rightarrow YH \text{ (protonation)} \tag{6}$$

The titrations were repeated three times and are represented by different symbols, showing good reproducibility. If this reaction proceeded stoichiometrically, and all the H^+ injected as HCl were consumed by the protonation of pAA, the apparent molar reaction enthalpy $Q_{m,app}$ would remain constant up to $C_H/C_Y = 1$, and the protonation enthalpy of pAA could be obtained as $\Delta H_{H,pAA}^{\circ} = -Q_{m,app}$ ($0 < C_H/C_Y < 1$). In reality, however, $Q_{m,app}$ is zero at the initial stage of the titration ($C_H = 0$), gradually becomes more negative, reaches an endothermic peak at $C_H/C_Y \approx 0.3$, and then decreases in magnitude until it returns to zero around $C_H/C_Y \approx 1.3$, where the endothermic protonation ends.

In order to examine whether the acid-base reaction of pAA is completely reversible, reverse titrations were also performed. Specifically, protonated pAA by the addition of excess HCl was titrated with sodium hydroxide. In this titration, the following reaction occurs:

$$YH + OH^- \rightarrow Y^- + H_2O \tag{7}$$

This reaction involves both the ionization (acid dissociation) of pAA (reaction 8) and the neutralization reaction of the solvent (reaction 9).

$$YH \rightarrow Y^- + H^+ \quad \text{(ionization)} \tag{8}$$

$$OH^- + H^+ \rightarrow H_2O \text{ (neutralization, in water)} \tag{9}$$

For the purpose of comparison with $Q_{m,app}$ for reaction (6), the corrected apparent molar heat of reaction $Q_{m,app}^{corr}$, calculated by the following equation, is plotted.

$$Q_{m,app}^{corr} = -\frac{q_i - q_{AP,i}}{C_T(v_i - v_{i-1})} \tag{10}$$

where $q_{AP,i}$ is the heat generated by neutralization, calculated using the $[H^+]$ at the i-th titration point ($[H^+]_i$), along with the autoprotolysis constant K_{AP} and the autoprotolysis enthalpy ΔH_{AP}°, as follows:

$$q_{AP,i} = -\Delta H_{AP}^{\circ} K_{AP}\left(\frac{v_i}{[H^+]_i} - \frac{v_{i-1}}{[H^+]_{i-1}}\right) \tag{11}$$

The negative sign in eq. (10) arises from the fact that reaction (7) involves the reverse of reaction (5). In Fig. 2, the $Q_{m,app}^{corr}$ values thus calculated are plotted using open symbols. As shown, they overlap with the filled symbols, which represent $Q_{m,app}$ for protonation. The agreement of the net enthalpograms obtained from both titration directions indicates that the acid-base equilibrium of pAA is a completely reversible reaction.

Hereafter, the discussion consistently refers to the ionization (acid dissociation) process to avoid confusion. Fig. 2 shows that the ionization of pAA is endothermic, with the endothermic peak at $C_H/C_Y \approx 0.3$, and the reaction continuing until $C_H/C_Y \approx 1.3$. This indicates that the ionization of pAA does not proceed stoichiometrically. A similar trend for CNp ionization has been reported, [29] as illustrated by cross symbols in Fig. 2. Although the C_H/C_Y ratio and the intensity of the endothermic peaks are different, the enthalpograms of pAA and CNp display similar behaviors. From these results, the hydration behavior in the vicinity of pAA on the CNp surface is concluded to be similar to that of isolated pAA in the bulk. Such $\Delta H_{a,pAA}^{\circ}$ values of a few kJ/mol, negative in sign and dependent on α, have been previously reported and discussed in detail [38], where they are attributed to enhanced hydration of the pAA chain

at a low degree of ionization. The surface pAA on CNp is therefore also likely to undergo enhanced hydration during the ionization process. However, equilibrium models were not successful in reproducing the enthalpogram.

A comparison of the ionization enthalpy with that of acetic acid is also of interest. There are several reported values for the ionization enthalpy of acetic acid, which are generally small, less than ±1 kJ/mol [39]. In our separate observation, exothermic ionization enthalpy of acetic acid was observed ($\Delta H_a^\circ = -0.3$ kJ/mol). Therefore, the endotherm observed in pAA (and CNp) is considered to be characteristic of polyelectrolytes, as suggested by the enhanced hydration of the pAA chain presented above. The ionization enthalpy of acetic acid ($\Delta H_{a,AcOH}^\circ$), along with that of pAA ($\Delta H_{a,pAA}^\circ$) and CNp ($\Delta H_{a,CNp}^\circ$) are summarized in Table 2.

3.2.2. In EAN

Fig. 3(a) shows the calorimetric titration curve of pAA in EAN. In this case, the sodium salt of pAA was titrated with TfOH in EAN. Therefore, the $Q_{m,app}$ observed in this titration corresponds to the heat of protonation of pAA (reaction 6). At the beginning, the heat of neutralization (of the solvent) was observed; subsequently, significant heat of protonation of pAA was generated during $0.5 < C_H/C_Y < 1.0$. This situation is markedly different from that in water, where the protonation is endothermic by a few kJ/mol. Assuming that the observed heats can be consistently explained by the protonation of pAA (reaction 6) and the neutralization (reaction 9, where $C_2H_5NH_2$ functions as the base instead of OH^- in EAN) the heat generated in the *i*-th titration point, $q_{r,i}$, can be expressed by using the ionization enthalpy of pAA, $\Delta H_{a,pAA}^\circ$, as follows:

$$q_{r,i} = \Delta H_{a,pAA}^\circ C_{Y,i} v_i (\alpha_i - \alpha_{i-1}) + q_{AP,i} \quad (12)$$

where $C_{Y,i}$ and α_i are the concentration of Y and the degree of ionization of pAA in the sample solution after *i*-th injection. The α_i values are calculated using equilibrium constants (β_0 and β_1) obtained by potentiometric titrations. The solid line represents the theoretical curve calculated using $\Delta H_{a,AP}^\circ = 80.5$ kJ/mol and $\Delta H_{a,pAA}^\circ = 31.5$ kJ/mol, which were determined by least-squares fitting. As shown, the calculated curve reproduces well the experimental data.

The ionization enthalpy of acetic acid in EAN has previously been reported to be greater ($\Delta H_{a,AcOH}^\circ = 30.6$ kJ/mol) than in water [40]. This was interpreted as the enthalpic cost associated with protonation of NO_3^- to form HNO_3, compared to that of H_2O to form H_3O^+. A similar interpretation can account for pAA: the greater $\Delta H_{a,pAA}^\circ$ value in EAN compared to that in water (a few kJ/mol negative $\Delta H_{a,pAA}^\circ$, as shown in Fig. 2) can be largely attributed to the solvent, rather than to a change in the ionization enthalpy of pAA. However, due to limitations in data accuracy, it remains unclear whether the unexplained exotherm peak that appears at H/Y = 0.3 in water also appears in EAN.

In summary, the ionization behavior of pAA in EAN resembles that in water. Significant differences in the ionization equilibrium and the ionization enthalpy primarily result from the process by which the solvent species receive H^+, and not from the process by which the carboxy groups of pAA release H^+.

Table 2
Ionization enthalpies of acetic acid (AcOH), pAA, and CNp in water (0.1 mol dm^{-1} NaCl), EAN and PIL18.

	AcOH	pAA	CNp
	$\Delta H_{a,AcOH}^\circ$ / kJ mol^{-1}	$\Delta H_{a,pAA}^\circ$ / kJ mol^{-1}	$\Delta H_{a,CNp}^\circ$ / kJ mol^{-1}
water	−0.3		
EAN	30.6	31.5	31
PIL18		33[a]	30[a,b]

a) Values are obtained within the titration ratio where reliable fitting was possible (see text). b) Ref. 29

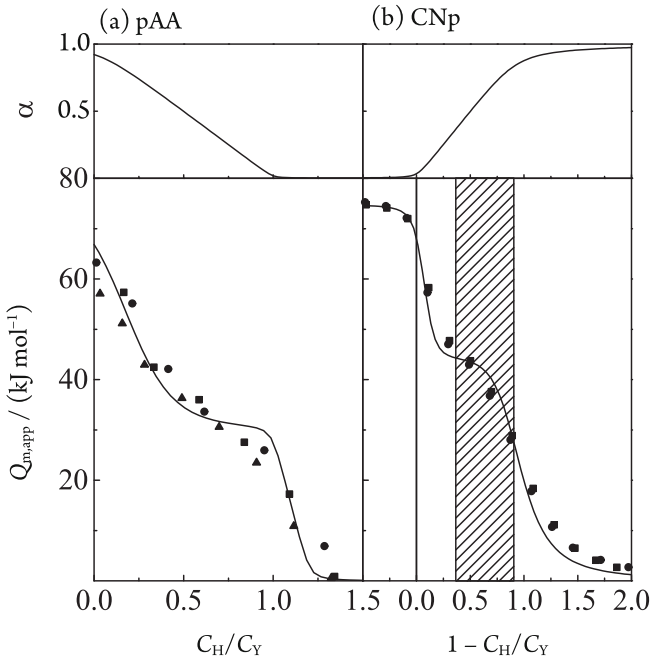

Fig. 3. Calorimetric titration curves of pAA and CNp in EAN, represented as the apparent molar heat of reaction, $Q_{m,app}$ (see text). (a) pAA sodium salt was titrated with an acidic EAN solution, and (b) acidic CNp dispersion was titrated with a basic EAN solution. Different symbol shapes indicate different repetitions of the titration. Above each titration curve, the corresponding degrees of dissociation (α) are shown.

The calorimetric titration curve of CNp in EAN is shown in Fig. 3(b). In this case, CNps were introduced into basic EAN, followed by the addition of excess TfOH to yield an acidic dispersion, which was then titrated with basic EAN using $C_2H_5NH_2$. The titration ratio is thus expressed as $1 - C_H/C_Y$, which increases as the titration proceeds. After the heat of neutralization, the ionization (acid dissociation) of YH occurred, and thus $Q_{m,app}$ corresponds to reaction 7 ($C_2H_5NH_2$ functions as the base instead of OH^-). The shaded area shows the region where flocculation was observed by potentiometry. Titration was repeated three times, which are represented by different symbols. The solid line is the theoretical curve using equilibrium constants (β_0 and β_1) obtained by potentiometry and the ionization enthalpy of CNp, $\Delta H_{a,CNp}^\circ = 31$ kJ/mol, determined by the least-squares fitting, exhibiting a good agreement with the experimental data. Since this value resembles the $\Delta H_{a,AcOH}^\circ$ and $\Delta H_{a,pAA}^\circ$ values in EAN, a similar interpretation seems to be valid for the CNp surface pAA. That is, no significant difference in the ionization process appears among acetic acid, isolated pAA, and CNp surface pAA.

3.2.3. Poly(acrylic acid)-coated nanoparticles in PIL18

Fig. 4 shows the calorimetric titration curve of pAA in PIL18. Sodium salt of pAA was introduced into acidic PIL18 by adding TfOH to yield a clear solution, which was then titrated with basic PIL18 using DEEA. Thus, the titration ratio is expressed as $1 - C_H/C_Y$, which increases as the titration proceeds. After the initial heat of neutralization, the ionization (acid dissociation) of YH occurred, where $Q_{m,app}$ corresponds to reaction (7). Titration was repeated three times, and good reproducibility was obtained. The solid line represents the theoretical curve calculated using equilibrium constants (β_0 and β_1) obtained by potentiometry and $\Delta H_{a,pAA}^\circ = 33$ kJ/mol. Unlike in EAN, the titration curve was not entirely reproduced in the range $0 < (1 - C_H/C_Y) < 0.3$, whereas the decrease in the heat of reaction at $0.3 < (1 - C_H/C_Y)$, in the course of pAA ionization, was well explained. Therefore, the least-squares fitting was conducted using the data in the range $(1 - C_H/C_Y) > 0.3$ to determine $\Delta H_{a,pAA}^\circ$.

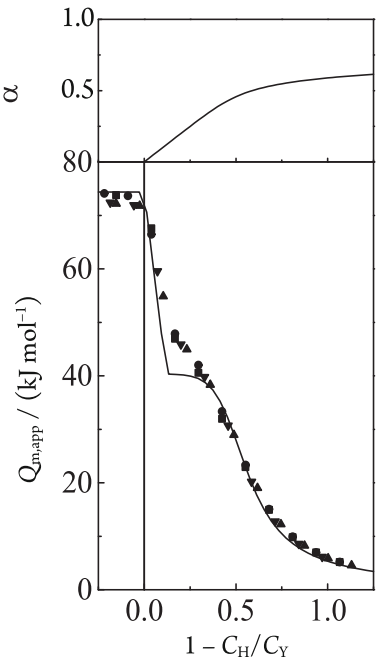

Fig. 4. Calorimetric titration curve of pAA in PIL18, represented as the apparent molar heat of reaction, $Q_{m,app}$ (see text). The corresponding degree of dissociation (α) is shown above the titration curve. Different symbol shapes indicate different repetitions of the titration.

The upward deviation in $Q_{m,app}$ from the theoretical curve at low values of $(1 - C_H/C_Y)$ indicates that excess heat that cannot be explained by the ionization process of CNp (reaction 7) is generated. We previously reported comparable excess heat during the ionization of CNp in PIL18, also observed in a similar C_H/C_Y region, with an estimated $\Delta H_{a,CNp}^{\circ}$ of 30 kJ/mol [29]. In contrast, the enthalpograms of both pAA and CNp can be explained by the ionization equilibria and enthalpies in EAN, as shown in Fig. 3. Therefore, this excess heat is characteristic solely of PIL18.

3.3. Polyelectrolytes behavior in ionic liquids

3.3.1. Hindrance of ionization at high degrees of dissociation

In all solvents, the ionization of both pAA and CNp is hindered at high degrees of dissociation due to the negative charges generated on pAA. Among the solvents studied, the hindrance is most pronounced in PIL18 compared to water and EAN, as indicated by the larger β_1 values. This is likely due to the bulky $DEEAH^+$, the counterion in PIL18, which prevents sufficient accumulation near the ionized pAA to effectively shield the negative charges. In contrast, relatively small cations in water and in EAN (Na^+ and $C_2H_5NH_3^+$, respectively) can approach the ionized pAA more easily and thereby provide effective electrostatic screening. In addition, the ionization enthalpies of pAA were found to be nearly consistent with those of acetic acid and CNp in each solvent. This implies that the difference in the hindrance effects between pAA and CNp in ionic liquids may be partly attributed to the conformational entropy of the pAA chains, [41,42] while it is difficult to discuss the respective entropic effects independently.

When the pH becomes sufficiently high and the degree of ionization increases, despite the intense ionic atmosphere of ionic liquids, CNp dispersions are stabilized likely due to the strong electrostatic repulsion between CNps in both PILs.

3.3.2. CNp dispersion at low degrees of ionization

A notable difference in the solvent dependence of the pH profile of CNp from that of pAA appears in the low-α region. As shown in Figs. 1(b) and 1(c), the ionization of CNp is promoted relative to pAA for α below 0.3–0.4. This is reflected in the more negative β_0 value of CNp than that of pAA (Table 1). The corresponding Gibbs energy can be estimated as $\Delta\Delta G_0 = RT(\ln 10)\,\beta_0$, giving $\Delta\Delta G_{0,CNp}^{EAN} = -5.1$ kJ/mol in EAN and $\Delta\Delta G_{0,CNp}^{PIL18} = -23.4$ kJ/mol in PIL18, indicating that CNp ionization undergoes some degree of stabilization. Considering that Gibbs energy consists of an enthalpic term and an entropic one ($\Delta G^{\circ} = \Delta H^{\circ} - T\Delta S^{\circ}$), and given that the ionization enthalpies of CNp and pAA are similar in respective solvents, it can be deduced that the favorable ionization of CNp is primarily driven by an entropic contribution.

The thermodynamic influence of the conformation of polyelectrolyte chains adsorbed on the nanoparticle surface on ionization was discussed in detail [41,42]. The extension of unionized pAA chains upon ionization was shown to reduce conformational freedom, which in turn suppresses ionization entropically, while the addition of salts mitigates this suppression. In the present CNp system, presumably, counterions are readily available in ionic liquids, thereby reducing the entropic cost and thus promoting the ionization of both pAA and CNp. When pH increases, CNps begin to aggregate, possibly sharing counterions, which leads to the release of excess cations into the bulk. This process is also entropically favorable. These two distinct entropic enhancements in ionization are specific to ionic liquids, probably because ionic liquids simultaneously play the roles of both solvent and counterion. This dual role gives rise to a mechanism that is completely different from colloidal stabilization in the aqueous phase (DLVO type, for instance), where ionization hinders aggregation consistently. This mechanism is illustrated in Scheme 1. This aggregation continues until further increase in pH leads to a higher charge density on the CNp surface, at which the shared counterions can no longer screen the electrostatic repulsion between CNps.

3.3.3. Polyelectrolytes in PIL18

As mentioned in Section 3.2.3, excess heats were observed during the ionization processes of pAA and CNp in PIL18, which cannot be explained solely by the ionization enthalpy of the carboxyl group. This observation was exclusive to PIL18 and thus contributes a decrease in $pK_{a,app}$. Since this effect appears in the low $1 - C_H/C_Y$ region (i.e., at low degrees of ionization), the enthalpic contribution primarily affects β_0, accounting for the more negative β_0 values in PIL18 than those in EAN. This enthalpic gain is presumably due to hydrogen-bonding interactions between the hydroxy groups of $DEEAH^+$ and pAA (or the surface pAA on CNps), rather than electrostatic interactions.

4. Conclusion

The behavior of polyelectrolytes (pAA) in PILs (EAN and PIL18) was elucidated through the thermodynamic functions of ionization. The ionization equilibrium of pAA was successfully described by expanding that of acetic acid using two parameters that represent (i) the promotion of ionization at the low degree of ionization (β_0) and (ii) the hindrance of the ionization with increasing the degree of ionization due to the charge inherent to pAA itself (β_1). This enables the quantitative comparison of ionization behavior of pAA in water and ionic liquids, excluding the contribution derived from the acid-base properties of the solvents. As a result, the differences in pAA ionization thermodynamics can be clearly highlighted. Regarding parameter (ii), the influence of the ionic liquids as electrolytes was evident. That is, the β_1 values for pAA in EAN showed a similar trend to that found in electrolyte aqueous solutions, indicating that EAN can screen the charge of ionized pAA, like conventional aqueous electrolyte solutions. In contrast, the ionization of pAA is significantly hindered in PIL18 as the charge of pAA increases, resulting in a large β_1 value. This suggests that the bulky PIL18 may weaken its role as an electrolyte. As for parameter (i), two different factors turn out to enhance ionization: an entropic factor accompanying ionization and flocculation in PILs for CNps and an enthalpic factor arising from hydrogen bonding with ionic liquid cations. With both factors at play in

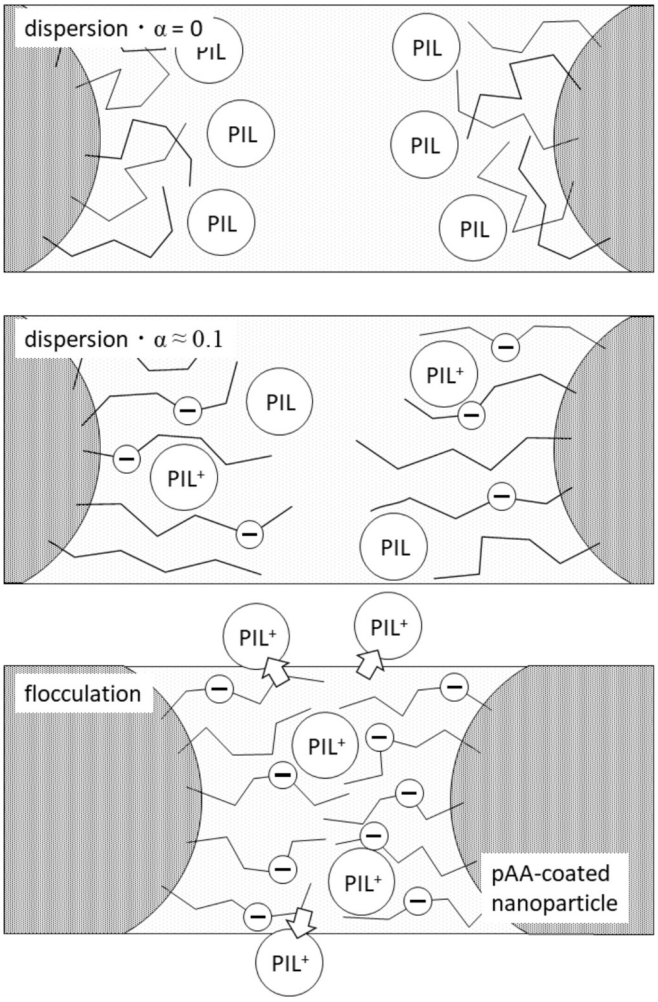

Scheme 1. Schematic illustration of CNp flocculation and counterion release. The aggregation induces the release of cationic counterions (PIL = EAN or PIL18, $PIL^+ = C_2H_5NH_3^+$ in EAN or $DEEAH^+$ in PIL18), resulting in an entropically favorable gain.

PIL18, the ionization of pAA on CNp at a low degree of dissociation is considerably promoted. Despite these differences, the enthalpy associated with the ionization process of carboxy group was found to be independent of the solvent, indicating that the local ionization mechanism of pAA and CNp is essentially the same as that of acetic acid monomer, both in aqueous and PIL environments.

The electrostatic effects at stake in the vicinity of charged particles may be one of the unique characteristics that distinguish ionic liquids from conventional solvents. This can be further elucidated by expanding the scope of ionic liquids. Besides, the interaction between polyelectrolytes and electrolytes in solvents is not yet fully understood. The combination of ionic liquids with highly charged particles such as pAA and CNp may contribute to deeper insight into these interactions. Although the present study focused on a single molecular weight of pAA, the chain length possibly influences the ionization behavior of polyelectrolytes, particularly through entropic contributions. The CNp size, which determines the surface curvature, may also affect the conformational response of pAA on the CNp surface to pH. Systematic investigations of these factors are expected to provide further insight into polyelectrolyte behavior in ionic liquids.

CRediT authorship contribution statement

Ryo Kanzaki: Writing – original draft, Project administration, Methodology, Investigation, Conceptualization. **Clément Guibert:** Writing – review & editing. **Jérôme Fresnais:** Writing – review & editing. **Véronique Peyre:** Writing – review & editing, Resources.

Declaration of competing interest

The authors declare that they have no known competing financial interests or personal relationships that could have appeared to influence the work reported in this paper.

Acknowledgement

This work was supported by JSPS KAKENHI Grant Numbers 21K05115 and 24H00782.

Data availability

Data will be made available on request.

References

[1] H.H. Ashassi-Sorkhabi, A. Kazempour, Application of Pitzer and six local composition models to correlate the mean ionic activity coefficients of aqueous 1-butyl-3-methylimidazolium bromide ionic liquid solutions obtained by EMF measurements, J. Chem. Thermodyn. 110 (2017) 71.
[2] C. Ma, A. Laaksonen, C. Liu, X. Lu, X. Ji, The peculiar effect of water on ionic liquids and deep eutectic solvents, Chem. Soc. Rev. 47 (2018) 8685.
[3] G. Perron, A. Hardy, J.-C. Justice, J.E. Desnoyers, Model system for concentrated electrolyte solutions: thermodynamic and transport properties of Ethylammonium nitrate in acetonitrile and in water, J. Solut. Chem. 22 (1993) 1159.
[4] M. Allen, D.F. Evans, R. Lumry, Thermodynamic properties of the ethylammonium nitrate+ water system: partial molar volumes, heat capacities, and expansivities, J. Solut. Chem. 14 (1985) 549.
[5] R. Kanzaki, H. Daiba, H. Kodamatani, T. Tomiyasu, Validation of pH standards and estimation of the activity coefficients of hydrogen and chloride ions in an ionic liquid, Ethylammonium nitrate, J. Phys. Chem. B 122 (2018) 10593–10599.
[6] R. Kanzaki, S. Uchida, H. Kodamatani, T. Tomiyasu, Copper (II) Chloro complex formation thermodynamics and structure in ionic liquid, 1-Butyl-3-Methylimidazolium Trifluoromethanesulfonate, J. Phys. Chem. B 121 (2017) 9659–9665.
[7] Daniel Himmel, Sascha K. Goll, Franziska Scholz, Valentin Radtke, Ivo Leito, Ingo Krossing, Absolute Brønsted acidities and pH scales in ionic liquids, Chem. Phys. Chem. Eur. J. 16 (2015) 1428.
[8] Valentin Radtke, Daniela Stoica, Ivo Leito, Filomena Camões, Ingo Krossing, Bárbara Anes, Matilda Roziková, Lisa Deleebeeck, Sune Veltzé, Teemu Näykki, Frank Bastkowski, Agnes Heering, Nagy Dániel, Raquel Quendera, Lokman Liv, Emrah Uysal, Nathan Lawrence, A unified pH scale for all solvents: part I – intention and reasoning (IUPAC technical report), Pure Appl. Chem. 93 (2021) 1049–1060.
[9] C.L. Bentley, A.M. Bond, J. Zhang, Voltammetric perspectives on the acidity scale and H^+/H_2 process in ionic liquid media, Annu. Rev. Anal. Chem. 11 (2018) 397–419.
[10] R. Kanzaki, H. Doi, X. Song, S. Hara, S. Ishiguro, Y. Umebayashi, J. Phys. Chem. B 116 (2012) 14146–14152.
[11] L.M. Mihichuk, G.W. Driver, K.E. Johnson, Brønsted acidity and the medium: fundamentals with a focus on ionic liquids, ChemPhysChem 12 (2011) 1622–1632.
[12] K.E. Johnson, R.M. Pagni, J. Bartmess, Brønsted acids in ionic liquids: fundamentals, organic reactions, and comparisons, Monatsh. Chem. 138 (2007) 1077–1101.
[13] J.A. Bautista-Martinez, L. Tang, J.-P. Belieres, R. Zeller, C.A. Angell, C. Friesen, Hydrogen redox in Protic ionic liquids and a direct measurement of proton thermodynamics, J. Phys. Chem. C 113 (2009) 12586–12593.
[14] Wu Xu Masahiro Yoshizawa, C. Austen Angell, Ionic liquids by proton transfer: vapor pressure, conductivity, and the relevance of ΔpK_a from aqueous solutions, J. Am. Chem. Soc. 126 (2003) 15411–15419.
[15] Z. He, P. Alexandridis, Ionic liquid and nanoparticle hybrid systems: emerging applications, Adv. Colloid Interf. Sci. 244 (2017) 54.
[16] Z. He, P. Alexandridis, Nanoparticles in ionic liquids: interactions and organization, Phys. Chem. Chem. Phys. 17 (2015) 18238.
[17] J.C. Riedl, M. Sarkar, T. Fiuza, F. Cousin, J. Depeyrot, E. Dubois a, G. Mériguet, R. Perzynski, V. Peyre, Design of concentrated colloidal dispersions of iron oxide nanoparticles in ionic liquids: structure and thermal stability from 25 to 200 °C, J. Colloid Interface Sci. 607 (2022) 584.
[18] Chandrabhan Verma, Eno E. Ebenso, M.A. Quraishi, Transition metal nanoparticles in ionic liquids: synthesis and stabilization, J. Mol. Liq. 276 (2019) 826.
[19] Susann Wegner, Christoph Janiak, Metal Nanoparticles in Ionic Liquids, Top. Curr. Chem. 375 (2017) 65.
[20] J.C. Riedl, M.A. Kazemi, F. Cousin, E. Dubois, S. Fantini, S. Lois, R. Perzynski, V. Peyre, Colloidal dispersions of oxide nanoparticles in ionic liquids: elucidating the key parameters, Nanoscale Adv. 2 (2020) 1560–1572.

[21] K. Bhattacharya, M. Sarkar, T.J. Salez, S. Nakamae, G. Demouchy, F. Cousin, E. Dubois, L. Michot, R. Perzynski, V. Peyre, Structural, Thermodiffusive and thermoelectric properties of Maghemite nanoparticles dispersed in Ethylammonium nitrate, Chem. Eng. 4 (2020) 5.
[22] M. Marium, M. Hoque, M.S. Miran, M.L. Thomas, I. Kawamura, K. Ueno, K. Dokko, M. Watanabe, Rheological and ionic transport properties of nanocomposite electrolytes based on Protic ionic liquids and silica nanoparticles, Langmuir 36 (2020) 148–158.
[23] P. Priyananda, H. Sabouri, N. Jain, B.S. Hawkett, Steric stabilization of γ-Fe2O3 superparamagnetic nanoparticles in a hydrophobic ionic liquid and the magnetorheological behavior of the Ferrofluid, Langmuir 34 (2018) 3068.
[24] M. Mamusa, J. Siriex-Plénet, F. Cousin, E. Dubois, V. Peyre, Tuning the colloidal stability in ionic liquids by controlling the nanoparticles/liquid interface, Soft Matter 10 (2014) 1097.
[25] L. Rodríguez-Arco, M.T. López-López, F. González-Caballero, J.D.G. Durán, Steric repulsion as a way to achieve the required stability for the preparation of ionic liquid-based ferrofluids, J. Colloid Interface Sci. 357 (2011) 252.
[26] N. Jain, X. Zhang, B.S. Hawkett, G.G. Warr, Stable and water-tolerant ionic liquid ferrofluids, ACS Appl. Mater. Interfaces 3 (2011) 662–667.
[27] R. Kanzaki, H. Kodamatani, T. Tomiyasu, H. Watanabe, Y. Umebayashi, A pH scale for the Protic ionic liquid Ethylammonium nitrate, Angew. Chem. Int. Ed. 55 (2016) 6266–6269.
[28] R. Kanzaki, C. Guibert, J. Fresnais, V. Peyre, Dispersion mechanism of polyacrylic acid-coated nanoparticle in protic ionic liquid, N, N-diethylethanolammonium trifluoromethanesulfonate, J. Colloid Interface Sci. 516 (2018) 248–253.
[29] R. Kanzaki, M. Sako, H. Kodamatani, T. Tomiyasu, C. Guibert, J. Fresnais, V. Peyre, Enthalpy profile of pH-induced flocculation and redispersion of polyacrylic acid-coated nanoparticles in protic ionic liquid, N,N-diethylethanolammonium trifluoromethanesulfonate, J. Mol. Liq. 349 (2022) 118146.
[30] R. Kanzaki, T. Hidaka, Y. Tokuda, H. Kodamatani, T. Tomiyasu, Brønsted acidity of bis(trifluoromethanesulfonyl)amide and trifluoromethanesulfonic acid in ionic liquids of ternary ammonium, J. Mol. Liq. 409 (2024) 125433.
[31] Yoshikazu Kawaguchi, Mitsuru Nagasawa, Potentiometric titration of stereoregular poly(acrylic acids), J. Phys. Chem. 73 (1969) 4382–4384.
[32] M. Mandel, The potentiometric titration of weak polyacids, Eur. Polym. J. 6 (1970) 807.
[33] I.T. Lucas, S. Durand-Vidal, E. Dubois, J. Chevalet, P. Turq, Surface charge density of Maghemite nanoparticles: role of electrostatics in the proton exchange, J. Phys. Chem. C 111 (2007) 18568.
[34] K.E. Brahmi, M. Rawiso, J. François, Potentiometric titration of acrylamide-acrylic acid copolymers: influence of the concentration, Eur. Polym. J. 29 (1993) 1531.
[35] A. Katchalsky, Problems in the physical chemistry of polyelectrolytes, J. Polym. Sci. 12 (1954) 159.
[36] C. Dolce, G. Mériguet, Ionization of short weak polyelectrolytes: when size matters, Colloid Polym. Sci. 295 (2017) 279.
[37] V.V. Annenkov, V.A. Kruglova, N.L. Mazyar, Analysis of the potentiometric titration curves within the framework of the theory of the neighbor effect, J. Polym. Sci. B Polym. Phys. 36 (1998) 931.
[38] V. Crescenzi, F. Delben, F. Quadrifoglio, D. Dolar, A comparative study of the enthalpy of ionization of Polycarboxylic acids in aqueous solution, J. Phys. Chem. 77 (1973) 539.
[39] J.J. Christensen, L. D. Hansen, R. M. Izatt, "Handbook of Proton Ionization Heats", John Wiley and Sons, New York, 1976.
[40] R. Kanzaki, H. Kodamatani, T. Tomiyasu, Proton thermodynamics in a Protic ionic liquid, Ethylammonium nitrate, Chem. Eur. J. 25 (2019) 13500–13503.
[41] R. Nap, P. Gong, I. Szleifer, Weak polyelectrolytes tethered to surfaces: effect of geometry, acid–base equilibrium and electrical permittivity, J. Polym. Sci. B Polym. Phys. 44 (2006) 2638.
[42] E.G. Solveyra, R.J. Nap, K. Huang, I. Szleifer, Theoretical modeling of chemical equilibrium in weak polyelectrolyte layers on curved Nanosystems, Polymers 12 (2020) 2282.